

Differentially rotating force-free magnetosphere of an aligned rotator: analytical solutions in split-monopole approximation

A. N. Timokhin*

*Physics Department, Ben-Gurion University of the Negev, POB 653, 84105 Beer-Sheva, Israel
Sternberg Astronomical Institute, Universitetskij pr. 13, 119992 Mocsow, Russia*

Accepted 2007 April 16, Received 2007 February 27; in original form 2007 February 27

ABSTRACT

In this paper we consider stationary force-free magnetosphere of an aligned rotator when plasma in the open field line region rotates differentially due to presence of a zone with the accelerating electric field in the polar cap of pulsar. We study the impact of differential rotation on the current density distribution in the magnetosphere. Using split-monopole approximation we obtain analytical expressions for physical parameters of differentially rotating magnetosphere. We find the range of admitted current density distributions under the requirement that the potential drop in the polar cap is less than the vacuum potential drop. We show that the current density distribution could deviate significantly from the “classical” Michel distribution and could be made almost constant over the polar cap even when the potential drop in the accelerating zone is of the order of 10 per cents of the vacuum potential drop. We argue that differential rotation of the open magnetic field lines could play an important role in adjusting between the magnetosphere and the polar cap cascade zone and could affect the value of pulsar breaking index.

Key words: stars:neutron – pulsars:general – MHD

1 INTRODUCTION

The physics of radiopulsars is still not fully understood despite large effort of many theoreticians in this field. It is generally assumed that radiopulsar has MHD-like magnetosphere which is very close to the force-free stage – the model firstly introduced by Goldreich & Julian (1969). For many years solution of force-free MHD equations was the problem, even for the simplest case of an aligned pulsar. Now to solve the Grade-Shafranov equation describing structure of a force-free magnetosphere of an aligned pulsar is not a problem anymore (see e.g. Contopoulos et al. 1999; Goodwin et al. 2004; Gruzinov 2005; Timokhin 2006). Stationary magnetosphere configurations for an aligned rotator were obtained also a the final stage in non-stationary numerical modelling (Komissarov 2006; McKinney 2006; Bucciantini et al. 2006; Spitkovsky 2006). Even the case of an inclined rotator was studied numerically (Spitkovsky 2006). However, the pulsar magnetosphere is a very complicated physical system because most of the current carriers (electrons and positrons) are produced inside the system, in the polar cap cascades. Production of electron-positron

pairs is a process with a threshold, so it could operate only under specific conditions and, generally speaking, not any given current density could flow through the cascade zone.

In magnetohydrodynamics (MHD) the current density distribution is not a free “parameter”, it is obtained in course of solving of MHD equations. In case of pulsars obtaining a solution of MHD equations does not solve the problem, because it could happen that the polar cap cascade zone could not provide the required current density distribution and, hence, support the particular configurations of the magnetosphere. In terms of MHD the polar cap cascade zone sets complicated boundary conditions at the foot points of the open magnetic field lines and any self-consistent solution of the problem must match them. The most “natural” configuration of the magnetosphere of an aligned rotator, when the last closed field line extends up to the light cylinder, requires current density distribution which could not be supported by stationary electromagnetic cascades in the polar cap of pulsar (see Timokhin 2006, hereafter Paper I). That configuration requires that in some parts of the polar cap the electric current flows against the preferable direction of the accelerating electric field. This seems to be not possible also for non-stationary cascades, although this problem requires more carefully investigation than it has been done before

* E-mail: atim@sai.msu.ru

(Fawley 1978; Al’Ber et al. 1975; Levinson et al. 2005). So, the structure of the magnetosphere should be different from this simple picture. The magnetosphere of a pulsar would have a configuration with the current density distribution which can flow through the polar cap cascade zone without suppression of electron-positron pair creation. Whether such configuration exists is still an open question, i.e. a possibility that the real pulsar magnetosphere has large domains where MHD approximation is broken could not be completely excluded too (see e.g. Arons 1979; Michel 1991).

As the pulsar magnetosphere and the polar cap cascade zone have too different characteristic timescales, it would be barely possible to proceed with modelling of the whole system at once. Therefore, these physical systems should be modelled separately and the whole set of solutions for each system should be found, in order to find compatible ones. Namely, we suggest the following approach to the construction of the pulsar magnetosphere model: one should find out which currents could flow through the force-free pulsar magnetosphere and compare them with the currents being able to flow through the polar cap cascade zone. In this work we deal with the first part of the the suggested “program”. Namely, we consider the range of possible current density distributions in force-free magnetosphere of an aligned rotator.

Force-free magnetosphere of an aligned rotator is the simplest possible case of an MHD-like pulsar magnetosphere and needs to be investigated in the first place. This system has two physical degrees of freedoms i) the size of the closed field line zone, and ii) the distribution of the angular velocity of open magnetic field lines. In each stationary configuration the current density distribution is fixed. Considering different configurations by changing (i) and (ii) and keeping them in reasonable range the whole set of admitted current density distributions can be found. Differential rotation of the open field lines is caused by variation of the accelerating electric potential in the cascade zone across the polar cap. Theories of stationary polar cap cascades predict rather small potential drop and in this case only one degree of freedom is left – the size of the zone with closed magnetic field lines. This case was studied in details in Paper I, with the results that stationary polar cap cascades are incompatible with stationary force-free magnetosphere. So, most probably the polar cap cascades operate in non-stationary regime. For non-stationary cascades the average potential drop in the accelerating zone could be larger than the drop maintained by stationary cascades. Hence, the open magnetic field lines may rotate with significantly different angular velocities even in magnetospheres of young pulsars. On the other hand, for old pulsars the potential drop in the cascade zone is large, and magnetospheres of such pulsars should rotate essentially differentially anyway.

The case of differentially rotating pulsar magnetosphere was not investigated in details before Although some authors addressed the case when the open magnetic field lines rotate differently than the NS, but only the case of constant angular velocity was considered (e.g. Beskin et al. 1993; Contopoulos 2005). The first attempt to construct a self-consistent model of pulsar magnetosphere with *differentially* rotating open field line zone was made in Timokhin (2007), hereafter Paper II. In that paper we considered only the case when the angular velocity of the open field lines is less than the an-

gular velocity of the NS. We have shown that the current density can be made almost constant over the polar cap, although on a cost of a large potential drop in the accelerating zone. The angular velocity distributions was chosen ad hoc and the analysis of the admitted range for current density distributions was not performed.

In this paper we discuss properties of differentially rotating magnetosphere of an aligned rotator in general and elaborate the limits on the differential rotation. We study in detail the case when the current density in the polar cap is a linear function on the magnetic flux. It allows us to obtain main relations analytically. We find the range in which physical parameters of the magnetosphere could vary, requiring that a) the potential drop in the polar cap is not greater than the vacuum potential drop and b) the current in the polar cap does not change its direction.

The plan of the paper is as follows. In Section 2 we discuss basic properties of differentially rotating force-free magnetosphere of an aligned rotator and derive equations for angular velocity distribution, current density and the Goldreich-Julian charge density in the magnetosphere. In Section 3 we derive equations for the potential drop which supports configurations with linear current density distribution in the polar cap of pulsar and give their general solutions. In Section 4 we analyse the physical properties of admitted magnetosphere configurations: the current density distribution, the maximum potential drop, the angular velocity of the open magnetic field lines, the Goldreich-Julian current density, the spindown rate and the total energy of the magnetosphere. At the end of that section we consider as examples two sets of solutions: the one with constant current densities and the another one with the smallest potential drops. In Section 5 we summarise the results, discuss limitation of the used approximation and briefly describe possible modification of the obtained solutions which will arise in truly self-consistent model. In that section we also discuss the issue with the pulsar braking index.

2 DIFFERENTIALLY ROTATING MAGNETOSPHERE: BASIC PROPERTIES

2.1 Pulsar equation

Here as in Papers I,II we consider magnetosphere of an aligned rotator that is at the coordinate origin and has dipolar magnetic field. We use normalisations similar¹ to the ones in Paper I, but now we write all equations in the spherical coordinates (r, θ, ϕ) . We normalise all distances to the light cylinder radius of the corotating magnetosphere $R_{LC} \equiv c/\Omega$, where Ω is the angular velocity of the neutron star (NS), c is the speed of light. For the considered axisymmetric case the magnetic field can be expressed through two dimensionless scalar functions Ψ and S as (cf. eq. (8) in Paper I)

$$\mathbf{B} = \frac{\mu}{R_{LC}^3} \frac{\nabla\Psi \times \mathbf{e}_\phi + S\mathbf{e}_\phi}{r \sin\theta}, \quad (1)$$

where \mathbf{e}_ϕ is the unit azimuthal, toroidal vector. $\mu = B_0 R_{NS}^3/2$ is the magnetic moment of the NS; B_0 is the magnetic field strength at the magnetic pole, R_{NS} is the NS

¹ note that here in contrast to Paper I Ψ is already dimensionless

radius. The scalar function Ψ is related to the magnetic flux as $\Phi_{\text{mag}}(\varpi, Z) = 2\pi (\mu/R_{\text{LC}}) \Psi(r, \theta)$. Φ_{mag} is the magnetic flux through a circle of a radius $\varpi = r \sin \theta$ with its centre at the point on the rotation axis being at the distance $Z = r \cos \theta$ from the NS. The lines of constant Ψ coincide with magnetic field lines. The scalar function S is related to the total current J outflowing through the same circle by $J(\varpi, Z) = 1/2 (\mu/R_{\text{LC}}^2) c S(r, \theta)$.

The electric field in the force-free magnetosphere is given by

$$\mathbf{E} = -\frac{\mu}{R_{\text{LC}}^3} \beta \nabla \Psi, \quad (2)$$

where β is the ratio of the angular velocity of the magnetic field lines rotation Ω_{F} to the angular velocity of the NS, $\beta \equiv \Omega_{\text{F}}/\Omega$ (cf. eq. (14) in Paper I). The difference of the angular velocity of a magnetic field line from the angular velocity of the NS is due to potential drop along that line in the polar cap acceleration zone.

For these dimensionless functions the equation describing the stationary force-free magnetosphere, the so-called pulsar equation (Michel 1973a; Scharlemann & Wagoner 1973; Okamoto 1974), takes the form (cf. eq. 20 in Paper I)

$$\begin{aligned} [1 - (\beta r \sin \theta)^2] \Delta \Psi - \frac{2}{r} \left(\partial_r \Psi + \frac{\cos \theta}{\sin \theta} \frac{\partial_\theta \Psi}{r} \right) + \\ + S \frac{dS}{d\Psi} - \beta \frac{d\beta}{d\Psi} (r \sin \theta \nabla \Psi)^2 = 0. \end{aligned} \quad (3)$$

This equation expresses the force balance across the magnetic field lines. At the light cylinder the coefficient by the Laplacian goes to zero and the pulsar equation reduces to

$$S \frac{dS}{d\Psi} = \frac{1}{\beta} \frac{d\beta}{d\Psi} (\nabla \Psi)^2 + 2\beta \sin \theta (\partial_r \Psi + \beta \cos \theta \partial_\theta \Psi). \quad (4)$$

Each smooth solution must satisfy these two equations and the problem of solving the pulsar equations transforms to an eigenfunction problem for the poloidal current function S (see e.g. Section 2.3 in Paper I). Equation (4) could also be considered as an equation on the poloidal current.

We adopt for the magnetosphere the configuration with the so-called Y-null point. Namely, we assume that the magnetosphere is divided into two zones, the first one with closed magnetic field lines, which extend from the NS up to the neutral point being at distance x_0 from the NS, and the second one, where magnetic field lines are open and extend to infinity (see Fig. 1). In the closed magnetic field line zone plasma corotates with the NS, there is no poloidal current along field lines, and the magnetic field lines there are equipotential. Apparently this zone can not extend beyond the light cylinder. In the rest of the magnetosphere magnetic field lines are open due to poloidal current produced by outflowing charged particles. The return current, needed to keep the NS charge neutral flows in a thin region (current sheet) along the equatorial plane and then along the last open magnetic field line. We assume that this picture is stationary on the time scale of the order of the period of the NS rotation. As it was outlined in Paper I, the polar cap cascades in pulsars are most probably non-stationary. The characteristic time scale of the polar cap cascades $\sim h/c \sim 3 \cdot 10^{-5}$ sec (h is the length of the acceleration zone being of the order of R_{NS}) is much shorter than the pulsar period (for most pulsars being $\gg 10^{-3}$ sec). So, for the global magnetosphere

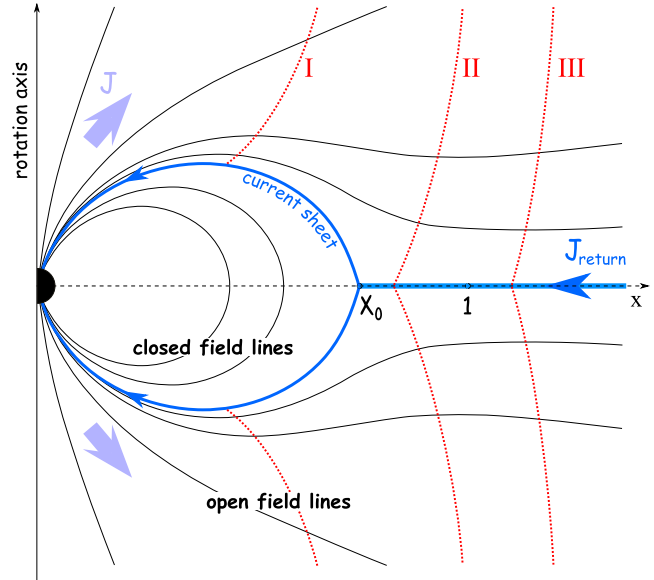


Figure 1. Structure of the magnetosphere of an aligned rotator (schematic picture). Magnetic field lines are shown by solid lines. Outflowing current J along open magnetic field lines and returning current J_{return} in the current sheet, separating the open and closed magnetic field line zones, are indicated by arrows. The current sheet is along the last open magnetic field line, corresponding to the value of the flux function Ψ_{pc} . Distances are measured in units of the light cylinder radius for the corotating magnetosphere R_{LC} , i.e. the point with $x = 1$ marks the position of the light cylinder in the corotating magnetosphere. The null point x_0 could lie anywhere inside the interval $[0, 1]$. Possible positions of the real light cylinder are shown by dotted lines. The line **I** corresponds to the case when $1/\beta(\Psi_{\text{pc}}) < x_0$; **II** – to $x_0 < 1/\beta(\Psi_{\text{pc}}) < 1$; **III** – to $1 < 1/\beta(\Psi_{\text{pc}})$ (see the text further in the article).

structure only time average of the physical parameters connected to the cascade zone are important. In the rest of the paper, when we discuss physical parameters set by the cascade zone we will always mean the *average* values of them, unless the opposite is explicitly stated.

Differential rotation of the open magnetic field lines which is caused by presence of a zone with the accelerating electric field in the polar cap of pulsar i) contributes to the force balance across magnetic field lines (the last term in eq.(3)), ii) modifies the current density in the magnetosphere (the first term in r.h.s. of eq. (4)), and iii) changes the position of the light cylinder, where condition (4) must be satisfied. Note that for the case i) and ii) the derivative $d\beta/d\Psi$, i.e. the form of the distribution $\beta(\Psi)$, plays an important role. So, for different angular velocity distributions in the open magnetic field line zone there should exist different magnetosphere configurations that have in general distinct current density distributions. Let us now consider restrictions on the differential rotation rate $\beta(\Psi)$.

2.2 Angular velocity of the open magnetic field lines

Due to rotation of the NS a large potential difference arises between magnetic field line foot points at the surface of the NS. The potential difference between the pole and the mag-

netic field line corresponding to the value of the magnetic flux function Ψ is

$$\Delta\mathcal{V}(\Psi) = \frac{\mu}{R_{\text{LC}}^2}\Psi \quad (5)$$

In perfectly force-free magnetosphere the magnetic field lines are equipotential. However, due to presence of the polar cap acceleration zone, where MHD conditions are broken a part of this potential difference appears as a potential drop between the surface of the NS and the pair-formation front, above which the magnetic field line remains equipotential. This potential drop is the reason why the open magnetic field lines rotate differently from the NS. The normalised angular velocity of a magnetic field line β is expressed through the potential drop along the field line as (e.g. Beskin (2005), Paper I)

$$\beta = 1 + \frac{R_{\text{LC}}^2}{\mu} \frac{\partial\mathcal{V}(\Psi)}{\partial\Psi}. \quad (6)$$

\mathcal{V} is the total potential drop (in statvolts) along the magnetic field line in the polar cap acceleration zone (cf. eq. (23) in Paper I).

The polar cap of pulsar is limited by the magnetic field line corresponding to a value of the flux function Ψ_{pc} . The potential drop between the rotation axis and the boundary of the polar cap is

$$\Delta\mathcal{V}(\Psi_{\text{pc}}) = \frac{\mu}{R_{\text{LC}}^2}\Psi_{\text{pc}} \equiv \Delta\mathcal{V}_{\text{pc}} \quad (7)$$

This is the maximum available potential drop along an open magnetic field line. It could be achieved in vacuum, when there is no plasma in the polar cap. We will call $\Delta\mathcal{V}_{\text{pc}}$ the vacuum potential drop. Let us normalise the poloidal flux function Ψ to its value at the last open magnetic field line Ψ_{pc} and introduce a new function $\psi \equiv \Psi/\Psi_{\text{pc}}$. Normalising potential drop along field lines to the vacuum potential drop and introducing the dimensionless function $V \equiv \mathcal{V}/\Delta\mathcal{V}_{\text{pc}}$ we rewrite expression for the normalised angular velocity of the open magnetic field line as

$$\beta = 1 + \frac{\partial V}{\partial\psi}. \quad (8)$$

As the potential drop *along* any field line can not be greater than the vacuum drop and could not have different sign than the vacuum drop, variation of the electric potential *across* the polar cap can not exceed the vacuum potential drop. In terms of the dimensionless functions this condition has the form

$$|V(\psi_1) - V(\psi_2)| \leq 1, \quad \forall \psi_1, \psi_2 \in [0, 1]. \quad (9)$$

Inequality (9) sets the limit on the electric potential in the polar cap of pulsar.

2.3 Current density in the polar cap

In order to obtain the current density distribution in the polar cap of pulsar the pulsar equation (3) together with the condition at the light cylinder (4) must be solved. There is an analytical solution of the pulsar equation only for split-monopole configuration of the poloidal magnetic field. Namely, when flux function Ψ has the form

$$\Psi = \Psi_{\text{M}}(1 - \cos\theta), \quad (10)$$

Ψ_{M} being a constant, equations (3) and (4) have a smooth solution if the poloidal current function S has the form (e.g. Blandford & Znajek 1977)

$$S(\Psi) = -\beta(\Psi)\Psi\left(2 - \frac{\Psi}{\Psi_{\text{M}}}\right). \quad (11)$$

Here Ψ_{M} corresponds to the value of the magnetic flux through the upper hemisphere, i.e. it corresponds to the magnetic field line lying in the equatorial plane. The poloidal current given by equation (11) is very similar to current in the well known Michel solution (Michel 1973b), but this expression is valid for non-constant $\beta(\Psi)$ too.

In this paper we will use for the poloidal current function S expression (11). Doing so, we assume that in the neighbourhood of the light cylinder the geometry of the poloidal magnetic field is close to a split monopole. This is good approximation if the size of the closed magnetic field line zone is much smaller than the light cylinder size, $x_0 \ll 1/\beta(\psi)$, $\psi < 1$. For configurations where the size of the corotating zone² approaches the light cylinder the poloidal current S is different from the one given by eq. (11), but we expect that this deviation should not exceed 10-20 per cents. Indeed, in the numerical simulations described in Paper I, where the case of constant $\beta \equiv 1$ was considered, the deviation of S from the Michel's poloidal current did not exceed 20 per cents and it got smaller for smaller size of the corotating zone (see Fig. 3 in Paper I). Similarly, in Paper II, where we considered the case of variable $\beta < 1$, the poloidal current deviated from the values given by the analytical formula (11) by less than 20 per cents and the difference became smaller for smaller size of the corotating zone. So, we may hope that the same relation holds in the general case too.

We intent to find the range of admitted current density distributions in the force-free magnetosphere. Here we use the split-monopole approximation for the poloidal current (11), hence, we can study only the effect of differential rotation on the current density distribution. The dependence of the current density on the size of the corotating zone in differentially rotating magnetosphere will be addressed in a subsequent paper, where we will refine our results by performing numerical simulations for different sizes of the corotating zone.

So, in our approximation the last closed field line in dipole geometry corresponds to the field line lying in the equatorial plane in monopole geometry, i.e. $\Psi_{\text{M}} = \Psi_{\text{pc}}$. In normalised variables expression for the poloidal current has the form

$$S(\Psi) = -\Psi_{\text{pc}}\beta(\psi)\psi(2 - \psi). \quad (12)$$

The poloidal current density in the magnetosphere is (see e.g. Beskin 2005)

$$j_{\text{pol}} = \frac{c}{4\pi} \frac{\mu}{R_{\text{LC}}^4} \frac{\nabla S \times \mathbf{e}_{\phi}}{r \sin\theta} = \frac{\Omega \mathbf{B}_{\text{pol}}}{2\pi c} c \frac{1}{2} \frac{dS}{d\Psi}. \quad (13)$$

In the polar cap of pulsar the magnetic field is dipolar and, hence poloidal. The Goldreich-Julian charge density for the

² plasma in the closed field line zone corotates with the NS, so we will call the region with the closed magnetic field lines the corotating zone

corotating magnetosphere near the NS is

$$\rho_{\text{GJ}}^0 = -\frac{\boldsymbol{\Omega} \cdot \mathbf{B}}{2\pi c}. \quad (14)$$

Using expressions (12)-(14) we get for the current density in the polar cap of pulsar

$$j = \frac{1}{2} j_{\text{GJ}}^0 [2\beta(1 - \psi) + \beta' \psi(2 - \psi)]. \quad (15)$$

The prime denotes differentiation with respect to ψ , i.e. $\beta' \equiv d\beta/d\psi$; $j_{\text{GJ}}^0 \equiv \rho_{\text{GJ}}^0 c$ is the Goldreich-Julian current density in the polar cap for the *corotating* magnetosphere. At the surface of the NS, where the potential drop is zero and plasma corotates with the NS, j_{GJ}^0 corresponds to the local GJ current density.

2.4 Goldreich-Julian charge density in the polar cap for differentially rotating magnetosphere

The Goldreich-Julian (GJ) charge density is the charge density which supports the force-free electric field:

$$\rho_{\text{GJ}} \equiv \frac{1}{4\pi} \boldsymbol{\nabla} \cdot \mathbf{E}. \quad (16)$$

The GJ charge density in points along a magnetic field line rotating with an angular velocity different from the angular velocity of the NS will be different from values given by the eq. (14). Substituting expression for the force-free magnetic field (2) into eq. (16) we get

$$\rho_{\text{GJ}} = -\frac{\mu}{4\pi R_{\text{LC}}^4} (\beta \Delta \Psi + \beta' (\nabla \Psi)^2). \quad (17)$$

We see that the GJ charge density depends not only on the angular velocity of the field line rotation (the first term in eq. (17)), but also on the angular velocity profile (the second term in eq. (17)).

Near the NS the magnetic field is essentially dipolar. The magnetic flux function Ψ for dipolar magnetic field is

$$\Psi^{\text{dip}} = \frac{\sin^2 \theta}{r}. \quad (18)$$

Substituting this expression into equation (17) we get

$$\rho_{\text{GJ}} = -\frac{\mu}{4\pi R_{\text{LC}}^4} \frac{1}{r^3} \times \left(\beta 2(3 \cos^2 \theta - 1) + \beta' \frac{\sin^2 \theta}{r} (3 \cos^2 \theta + 1) \right). \quad (19)$$

In the polar cap of pulsar $\cos \theta \simeq 1$ and $\mu/(r R_{\text{LC}})^3 \simeq B/2$. Recalling expression for the magnetic flux function for dipole magnetic field (18) we get for the local GJ charge density in the polar cap of pulsar

$$\rho_{\text{GJ}} = \rho_{\text{GJ}}^0 (\beta + \beta' \psi). \quad (20)$$

3 ACCELERATING POTENTIAL

In our approximation any current density distribution in force-free magnetosphere of an aligned rotator has the form given by eq. (15). The current density depends on the angular velocity of the magnetic field lines $\beta(\psi)$, which for a given field line depends on the total potential drop along

that line via equation (8). The potential drop in the acceleration zone can not exceed the vacuum potential drop, i.e. V is limited by inequality (9).

So, if we wish to find the accelerating potential which supports a force-free configuration of the magnetosphere for a given form of the current density distribution³ in the polar cap we do the following. We equate the expression for the current density distribution to the general expression for the current density (15), then we express $\beta(\psi)$ in terms of $V(\psi)$ by means of equation (8), and obtain thus an equation for the electric potential V which supports a force-free magnetosphere configuration with the desired current density distribution. If solutions of the obtained equation fulfill limitation (9), such configuration is admitted, if not – such current density could not flow in force-free magnetosphere of an aligned pulsar. Currently there is no detailed model for non-stationary polar cap cascades from which we could deduce reasonable shapes for current density distribution. Therefore, we try to set constrains on the current density assuming linear dependence of the current density on ψ .

In differentially rotating magnetosphere there are two characteristic current densities. The first one is the Goldreich-Julian current density for the corotating magnetosphere j_{GJ}^0 . It corresponds to the actual Goldreich-Julian current density in the magnetosphere at the NS surface, where differential rotation is not yet build up. The second characteristic current density is the actual Goldreich-Julian current density j_{GJ} in points above the acceleration zone where the magnetosphere is already force-free and the final form of differential rotation is established; in the polar cap j_{GJ} is given by formula (20). For magnetosphere with strong differential rotation the current densities j_{GJ}^0 and j_{GJ} differ significantly. In this section we consider both cases, namely, when the current density distribution is normalised to j_{GJ}^0 and when it is normalised to j_{GJ} .

3.1 Outflow with the current density being a constant fraction of the actual Goldreich-Julian current density

For non-stationary cascades the physics would be determined by the response of the cascade zone to the inflowing particles and MHD waves coming from the magnetosphere. However, the accelerating electric field depends on the deviation of the charge density from the local value of the GJ charge density. So, the first naive guess would be that the preferable state of the cascade zone would be the state when (on average) the current density is equal to the GJ current density j_{GJ} :

$$j(\psi) = j_{\text{GJ}}(\psi) = j_{\text{GJ}}^0 (\beta + \beta' \psi). \quad (21)$$

Equating this formula to the general expression for the current density (15) and substituting for β expression (8), after algebraical transformation we get the equation for the accelerating electric potential in the polar cap of pulsar

$$V'' = -2 \frac{1 + V'}{\psi}. \quad (22)$$

We set the boundary conditions for V at the edge of the polar cap. As the boundary conditions we can use the value

³ guessed from a model for the polar cap cascades, for example

of the normalised angular velocity at the edge of the polar cap and the value of the electric potential there

$$1 + V'(1) = \beta_{\text{pc}} \quad (23)$$

$$V(1) = V_0 \quad (24)$$

Solution of equation (22) satisfying the boundary conditions (24), (23) is

$$V(\psi) = V_0 + (1 - \psi) \left(1 - \frac{\beta_{\text{pc}}}{\psi} \right). \quad (25)$$

We see that unless $\beta_{\text{pc}} = 0$ the potential has singularity at the rotation axis, and, hence, such configuration can not be realised in force-free magnetosphere of a pulsar. The condition (9) is violated – the potential difference exceeds the vacuum potential drop.

If $\beta_{\text{pc}} = 0$, the potential is $V = V_0 + 1 - \psi$ and from eq. (8) we have $\beta(\psi) \equiv 0$. Substituting this into eq. (15) we get for the current density $j(\psi) \equiv 0$. So, the case with $\beta_{\text{pc}} = 0$ is degenerated, as there is no poloidal current in the magnetosphere, it corresponds to the vacuum solution.

Let us consider now a more general form for the current density distribution

$$j(\psi) = A j_{\text{GJ}}(\psi) = A j_{\text{GJ}}^0 (\beta + \beta' \psi), \quad (26)$$

where A is a constant. In that case for the accelerating electric potential in the polar cap of pulsar we have the equation

$$V'' = 2(1 + V') \frac{1 - A - \psi}{\psi [2(A - 1)]} \quad (27)$$

For the same boundary conditions (24), (23) solution of this equation is

$$V(\psi) = V_0 + 1 - \psi + \frac{\beta_{\text{pc}}(2A - 1)}{2(A - 1)} \log \left[\frac{\psi(2A - 1)}{\psi + 2(A - 1)} \right]. \quad (28)$$

This solution is valid for $A \neq 1, 1/2$. There is the same problem with the electric potential in that solution. Namely, unless $\beta_{\text{pc}} = 0$ the potential V is singular⁴ at the rotation axis. The case with $A = 1/2$ is also degenerated, because in that case the solution for the electric potential is $V(\psi) = V_0 + 1 - \psi$ what yield the current density $j(\psi) \equiv 0$.

We see that solutions with the current density being a constant fraction of the actual GJ current density are not allowed, except a trivial degenerated case, corresponding to no net particle flow. The naive physical picture does not work and the current density in the magnetosphere in terms of the actual GJ current density must vary across the polar cap. On the other hand, the GJ current density is itself a variable function across the polar cap, it changes also with the altitude within the acceleration zone, when the potential drop increases until it reaches its final value. So, we find it more convenient to consider the current density in terms of the corotational GJ current density.

3.2 Outflow with the current density being a linear function of the magnetic flux in terms of the corotational Goldreich-Julian current density

In models with the space charge limited flow (SCLF), when charged particles can freely escape from the NS surface (e.g. Scharlemann et al. 1978), the charge density at the NS surface is always equal to the local GJ charge density there, ($\rho = \rho_{\text{GJ}}^0|_{r=R_{\text{NS}}}$). For SCLF the actual current density in the polar cap could be less than j_{GJ}^0 if acceleration of the particles is periodically blocked in the non-stationary cascades. The current density could be greater than j_{GJ}^0 if there is an inflow of particles having opposite charge to that of the GJ charge density from the magnetosphere into the cascade zone (e.g. Lyubarskij 1992). Therefore, an expression for the current density in terms of the corotational GJ current density j_{GJ}^0 would be more informative from the point of view of the cascade physics.

Let us consider the case when the current density distribution in the polar cap of pulsar has the form

$$j = j_{\text{GJ}}^0 (a\psi + b), \quad (29)$$

where a, b are constants. The Michel current density distribution is a particular case of this formula and corresponds to the values of parameters $a = -1, b = 1$. The equation for the electric potential for this current density is

$$V'' = 2 \frac{a\psi + b - (1 + V')(1 - \psi)}{\psi(2 - \psi)}. \quad (30)$$

Solution of the equation (30) satisfying the boundary conditions (24), (23) is

$$V(\psi) = V_0 + (1 + a)(1 - \psi) + \frac{1}{2} \log \left[(2 - \psi)^{-\beta_{\text{pc}} - 3a - 2b} \psi^{\beta_{\text{pc}} - a - 2b} \right]. \quad (31)$$

We see that the potential is non singular at the rotation axis, if $\beta_{\text{pc}} = a + 2b$. So, the admitted solution for the electric potential is

$$V(\psi) = V_0 + (1 + a)(1 - \psi) - 2(a + b) \log(2 - \psi). \quad (32)$$

In the rest of the paper we will use for the electric potential expression (32). We will analyse physical properties of force-free magnetosphere configurations when the electric potential in the acceleration zone of the polar cap has that form.

4 PROPERTIES OF ADMITTED CONFIGURATIONS

4.1 Admitted current density

The potential drop in the polar cap of pulsar is limited by the vacuum potential drop. In our notations this limit is formulated as inequality (9). Parameters a, b from the expression for the electric current (29) enters into the formula for the electric potential (32). Imposing limitation (9) we get the admitted range for these parameters in the force-free magnetosphere. In Appendix A we do such analysis and find the region in the plane (a, b) which is admitted by the requirement (9). This region is shown as a grey area in Fig. A1.

⁴ the singularity arises because $V''(0)$ goes to infinity unless $1 + V'(0) = \beta(0)$ is zero, as it follows from equation (27)

From Fig. A1 it is evident that for the most of the admitted values of parameters a, b the current density has different signs in different parts of the polar cap. There is also a region where the values of parameters correspond to the current density distributions having the same sign as the GJ charge density in the whole polar cap.

The physics of the polar cap cascades impose additional limitations on the current density and accelerating electric potential distribution in the polar cap. There is now no detailed theory of non-stationary polar cap cascades. Therefore, in setting constraints on the current density distribution we should use some simple assumptions about the possible current density. There is a preferable direction for the accelerating electric field in the polar cap. The direction of this field is such that it accelerates charged particles having the same sign as the GJ charge density away from the star. It is natural to assume that the average current in the polar cap cascade should flow in the same direction. The average current could flow in the opposite direction only if the accelerating electric field is screened. In order to screen the accelerating field a sufficient amount of particles of the same sign as the accelerated ones should come from the magnetosphere and penetrate the accelerating potential drop. These particles, however, are themselves produced in the polar cap cascade. They must be accelerated somewhere in the magnetosphere back to the NS up to the energy comparable with the energy the primary particles get in the polar cap cascade. Even if the problem of particle acceleration back to the NS could be solved, screening of the electric field will interrupt the particle creation, and, hence, there will be not enough particles in the magnetosphere which could screen the electric field the next time. Although the real physics is more complicated and is not yet fully understood, the case of the unidirectional current in the polar cap is worth of detailed investigation as it is “the most natural” from the point of view of the polar cap cascade physics. In the following we will call the current being of the same sign as the GJ charge density as “positive” and the current being of the opposite sign to the GJ charge density as “negative”.

The linear current density distribution (29) will be always positive if

$$b \geq \max(-a, 0). \quad (33)$$

Only a subset of the admitted values of a, b corresponds to the positive current density distribution. Such values of the parameters a, b are inside the triangle-like region shown in Figs. 2, 3, 4. We see that a rather wide variety of positive current density distributions are admitted in the force-free magnetosphere: current density distributions being constant across the polar cap of pulsar are admitted, as well as current densities decreasing or increasing toward the polar cap boundary. So, the current density in the force-free magnetosphere could deviate strongly from the classical Michel current density, corresponding to the point $a = -1, b = 1$. The price for this freedom is the presence of a non-zero accelerating electric potential in the polar cap. If the price for a particular current density distribution is too high, i.e. if the potential drop is too large, only magnetosphere of pulsars close to the “death line” could admit such current density. Let us now consider the distribution of the potential drop in the parameter space (a, b) .

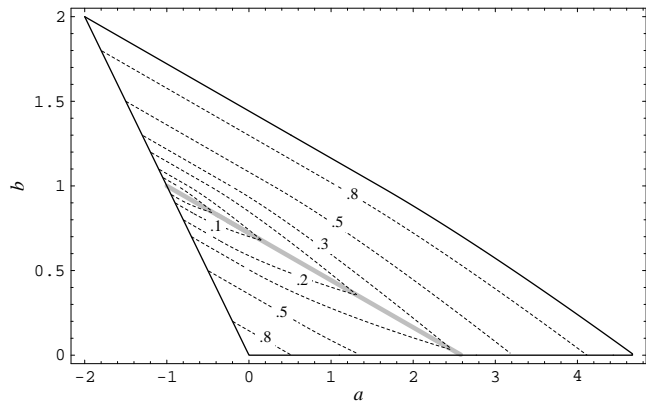


Figure 2. Maximum potential drop across the polar cap. The dotted lines show contours of ΔV_{\max} . Contours for $\Delta V_{\max} = 0.05, 0.1, 0.2, 0.5, 0.8$ are shown. Labels on the lines correspond to the values of ΔV_{\max} . The line corresponding to $\Delta V_{\max} = 0.05$ is not labelled.

4.2 Electric potential

We emphasised already that the shape of the function $V(\psi)$ is very important for the resulting current density distribution. However, as we do not understand in detail the physics of non-stationary cascades, we cannot judge whether a particular form of $V(\psi)$ is admitted by the cascade physics or not. On the other hand, in young pulsars the average potential drop could not be very large, because already a small fraction of the vacuum potential drop would be sufficient for massive pair creation and screening of the accelerating electric field. So, currently we could judge about reasonableness of a particular current density distribution only from the maximum value of the potential drop it requires. The electric potential given by eq. (32) is known up to the additive constant V_0 , which is the value of the accelerating potential at the polar cap boundary. V_0 and thus the actual potential drop in the accelerating zone can not be inferred from the magnetosphere physics and is set by the physics of the polar cap cascades. The only thing we could say about the actual potential drop in the acceleration zone *along* field lines is that its absolute value is not smaller than the absolute value of the maximum potential drop of $V(\psi)$ *across* the polar cap.

Let us now consider possible values of the maximum potential drop across the polar cap of pulsar. If the potential is a monotone function of ψ in the polar cap, the maximum potential drop is the drop between the rotation axis and the polar cap boundary. If the potential as a function of ψ has a minimum inside the polar cap, the maximum potential drop will be either between the axis and the minimum point, or between the edge and the minimum point. We analyse this issue in details in Appendix B. In Fig. 2 the contour map of the maximum potential drop in the plane (a, b) is shown. The line given by eq. (B1) is the line where for fixed a (or b) the smallest value of the potential drop across the polar cap is achieved. From this plot it is evident that even if the potential drop in the polar cap is rather moderate, of the order of ~ 10 per cents, there are force-free magnetosphere configurations with the current density distribution deviating significantly from the Michel current density distribution.

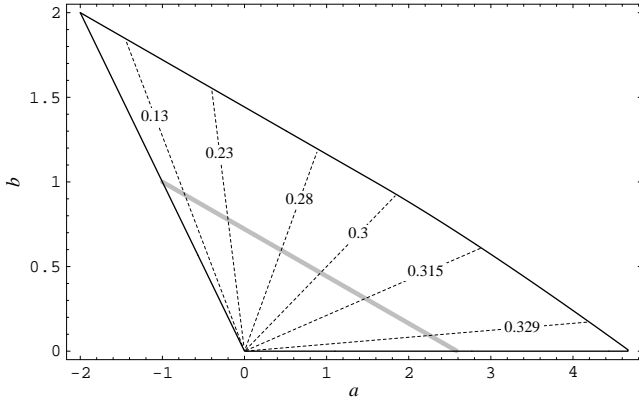


Figure 3. Ratio of the actual current density to the Goldreich-Julian current density $\iota(1)$ at the polar cap boundary, where the minimum value of this ratio is achieved, see text. The dotted lines show contours of $\iota(1)$

So, even for young pulsars there may be some flexibility in the current density distribution admitted by the force-free electro-dynamics.

Note that force-free magnetosphere impose different constraints on pulsars in aligned $\boldsymbol{\mu} \cdot \boldsymbol{\Omega} > 0$ and anti-aligned configuration $\boldsymbol{\mu} \cdot \boldsymbol{\Omega} < 0$ configuration (pulsar and antipulsar in terms of Ruderman & Sutherland (1975)). For pulsars the accelerating potential is positive, i.e. it increases from the surface of the NS toward the force-free zone above the pair formation front. In case of antipulsar the potential is negative, it decreases toward the pair formation front, because positive charges are accelerated. Equations for the current density (15), (29) we used to derive the equation for the electric potential (30) contain the expression for the GJ charge density as a factor, and, hence, the resulting expression for the electric potential is the same for each sign of the GJ current density. So, for pulsars there is a *minimum* in the accelerating potential distribution, for antipulsar the distribution of the accelerating electric potential has a *maximum*. Mathematically this results from different signs of the integration constant V_0 .

4.3 Angular velocity

The normalised angular velocity of the open magnetic field lines in the force free magnetosphere with linear current density distribution (29) is given by

$$\beta(\psi) = \frac{2b + a\psi}{2 - \psi}. \quad (34)$$

For admitted current densities it grows with increasing of ψ , because the first derivative $d\beta/d\psi$ for the admitted values of a, b is always non-negative. So, the angular velocity either *increase* toward the polar cap boundary or remains *constant* over the cap if $a = -b$. The latter case includes also the Michel solution. The minimum value of β

$$\beta_{\min} = b, \quad (35)$$

is achieved at the rotation axis, where $\psi = 0$, and the maximum value

$$\beta_{\min} = 2b + a, \quad (36)$$

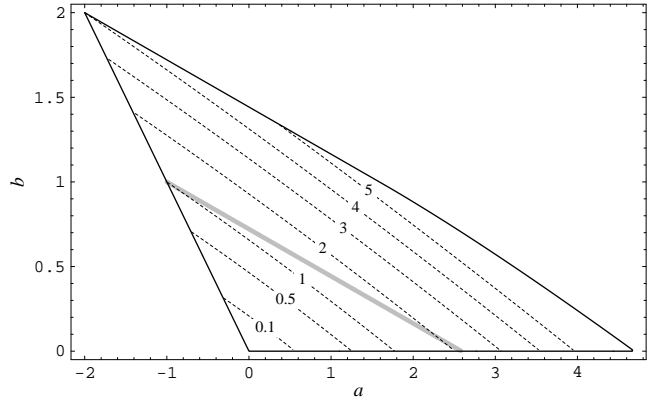


Figure 4. Spindown rate in terms of the Michel spindown rate. Dotted lines show contours of w . Label on the lines correspond to the values of w .

at the polar cap boundary, where $\psi = 1$. So, the open field lines can rotate slower, as well as faster than the NS, but the lines near the polar cap boundary rotate not slower than the lines near the rotation axis.

4.4 Goldreich-Julian current density

Expression for the GJ current density in the polar cap can be obtained by substitution of the expression (34) for β into equation (20) for the GJ current density. We get

$$j_{\text{GJ}}(\psi) = j_{\text{GJ}}^0 \frac{4b + a\psi(4 - \psi)}{(\psi - 2)^2}. \quad (37)$$

For the admitted values of the parameters a, b the derivative $dj_{\text{GJ}}/d\psi$ is always non-negative and, hence, the GJ current density either *increases* toward the polar cap boundary, or remains *constant* when $a = -b$. The actual current density, however, could decrease as well as increase toward the polar cap edge.

For the charge separated flow the deviation of the current density from the GJ current density generate an accelerating or a decelerating electric field when $j < j_{\text{GJ}}$ or $j > j_{\text{GJ}}$ correspondingly. Although in non-stationary cascades the particle flow would be not charge separated, the ratio of the actual current density to the GJ current density may give some clues about cascade states required by a particular magnetosphere configuration. This ratio is given by

$$\iota(\psi) \equiv \frac{j(\psi)}{j_{\text{GJ}}(\psi)} = \frac{(\psi - 2)^2(b + a\psi)}{a\psi(4 - \psi) + 4b} \quad (38)$$

For each admitted configuration the current density is equal to the GJ current density at the rotation axis. For the admitted values of the parameters a, b the derivative $d\iota/d\psi$ is always positive, and, hence, the current density in terms of the GJ current density *decreases* toward the polar cap boundary. So, except the rotation axis the current density in the polar cap is always less than the GJ current density. The relative deviation of the actual current density from the GJ current density is maximal at the polar cap boundary

$$\iota(1) = \frac{a + b}{3a + 4b}. \quad (39)$$

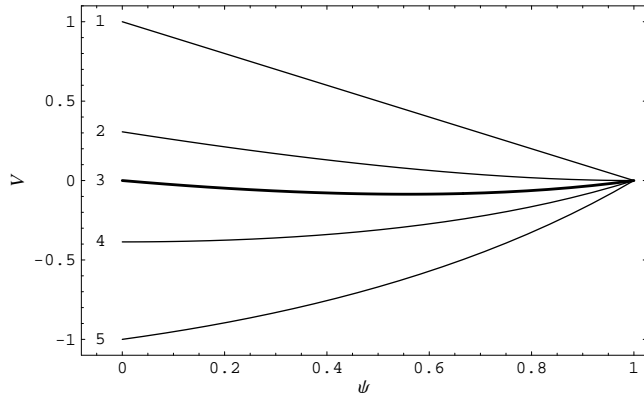


Figure 5. Electric potential in the polar cap of pulsar as a function of the normalised flux function ψ for magnetosphere configurations with a constant current density across the cap. In all cases V_0 is set to zero. Numbers near the lines correspond to the following values of b : 1 — $b = 0$; 2 — $b = .5$; 3 — $b = b_{\max}/2$; 4 — $b = 1$; 5 — $b = b_{\max}$. The line corresponding to the minimum potential drop across the cap is shown by the thick solid line (the line 3).

Its maximum value $\iota_{\max} = 1/3$ this ratio achieves when $b = 0$. Its minimum value $\iota_{\min} = 0$ it achieves when $a = -b$, what includes also the case of the Michel’s current density distribution. The contours of $\iota(1)$ are shown in Fig. 3.

4.5 Spin-down rate and the total energy of electromagnetic field in the magnetosphere

In our notations the spindown rate of an aligned rotator is (cf. eq. (60) in Paper I)

$$W = W_{\text{md}} \int_0^{\Psi_{\text{pc}}} S(\Psi) \beta(\Psi) d\Psi, \quad (40)$$

where W_{md} is the magnetodipolar energy losses defined as

$$W_{\text{md}} = \frac{B_0^2 R_{\text{NS}}^6 \Omega^4}{4c^3}. \quad (41)$$

Substituting expression for the poloidal current (12) and using the normalised flux function ψ we get

$$W = W_{\text{md}} \Psi_{\text{pc}}^2 \int_0^1 \beta^2(\psi) \psi(2-\psi) d\psi. \quad (42)$$

Expression for the spindown rate in the Michel solution

$$W_{\text{M}} = \frac{2}{3} \Psi_{\text{pc}}^2 W_{\text{md}} \quad (43)$$

differs from the spindown rate obtained in the numerical simulations of the corotating aligned rotator magnetosphere with by a constant factor. However, it has very similar dependence on the size of the corotating zone x_0 (cf. equations (62), (63) in Paper I). As our solutions are obtained in split-monopole approximation, they should differ from the real solution approximately in the same way as the Michel solution does. Because of this it would be more appropriate to normalise the spindown rate to the spindown rate in the Michel split-monopole solution. Doing so we will be able to study the effect of differential rotation on the energy losses separately from the dependence of the spindown rate on the size of the corotating zone.

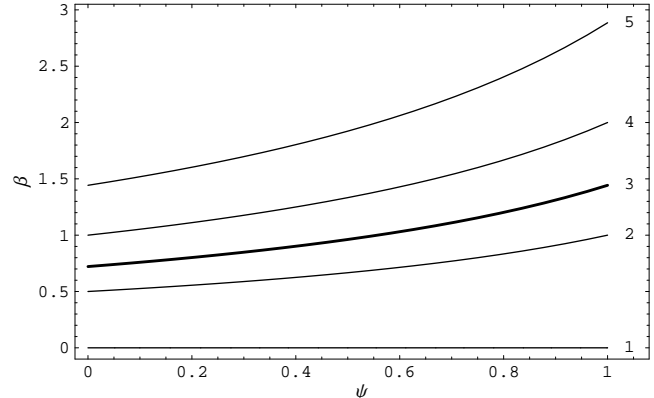


Figure 6. Normalised angular velocity of the open magnetic field lines as a function of the normalised flux function ψ for magnetosphere configurations with a constant current density across the cap. Labelling of the curves is the same as in Fig. 5.

For the normalised spindown rate in the considered case of linear current density we get

$$w \equiv \frac{W}{W_{\text{M}}} = 4a^2(3 \log 2 - 2) + 3ab(8 \log 2 - 5) + 6b^2(2 \log 2 - 1). \quad (44)$$

In Fig. 4 contour lines of w are shown in the domain of admitted values for parameters a, b . We see that spindown rate can vary significantly, from zero to the value exceeding the Michel’s energy losses by a factor of ≈ 6 . It increases with increasing of the values of the parameters a, b and decreases with decreasing of that values. It is due to increasing or decreasing of the total poloidal current in the magnetosphere correspondingly.

The total energy of the magnetosphere could be estimated from the split-monopole solution. Using the formula (C7) derived in Appendix C we have for the total energy of the electromagnetic field

$$\mathcal{W} \simeq \mathcal{W}_{\text{pol}} + (R - R_{\text{NS}}) W, \quad (45)$$

where \mathcal{W}_{pol} is the total energy of the poloidal magnetic field and R is the radius of the magnetosphere. The first term in our approximation is the same for all magnetosphere configurations, the difference in the total energy arises from the second term. Hence, the contours of the constant total energy in the plane (a, b) have the same form as the contours of the spindown rate W shown in Fig. 4. So, the total energy of the magnetosphere increases with increasing of parameters a, b , i.e. it increases with the increase of the poloidal current.

4.6 Example solutions

As examples we consider here the properties of two particular solutions in details. We chose these solution because either their current density or the potential drop seem to correspond to “natural” states of the polar cap cascades. Although we do not claim that one of the solutions is realised as a real pulsar configuration, but knowledge of their properties may be helpful in understanding of the physical conditions the polar cap cascades should adjust to.

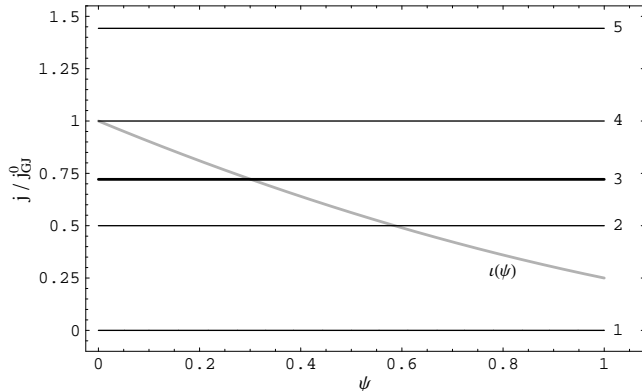


Figure 7. Current density as a function of the normalised flux function ψ for magnetosphere configurations with a constant current density across the cap. Labelling of the curves is the same as in Fig. 5. By the thick grey line the ratio of the actual current density to the GJ current density $i(\psi)$ is shown. For this case it is the same for all solutions.

4.6.1 Configurations with constant current density

At first we consider the case when the current density is constant over the polar cap, i.e. $a = 0$ and $j = b j_{\text{GJ}}^0$. Constant density distribution would be produced by cascades in their “natural” state, if the current adjustment proceeds locally, without strong influence from the current along adjacent field lines. The electric potential in that case is

$$V^c(\psi) = V_0 + 1 - \psi - 2b \log(2 - \psi). \quad (46)$$

This potential has the following properties (see Fig. 5 where $V(\psi)$ is shown for several values of b assuming for the sake of simplicity $V_0 = 0$):

- the admitted values of the current density in the polar cap of pulsar are within interval $[0, b_{\text{max}}]$, where $b_{\text{max}} = 1/\log 2 \simeq 1.443$.
- if $0 < b < b_{\text{max}}/2 \simeq 0.721$ the value of the electric potential at the rotation axis $V^c(0)$ is larger than that value at the polar cap edge $V^c(1)$, $V^c(0) > V^c(1)$
- if $b_{\text{max}}/2 < b < b_{\text{max}}$ the value of the electric potential at the rotation axis $V^c(0)$ is smaller than that value at the polar cap edge $V^c(1)$, $V^c(0) < V^c(1)$.
- if $0 < b < 1/2$ or $1 < b < b_{\text{max}}$ the potential is a monotone function of ψ ; if $1/2 < b < b_{\text{max}}$ it has a minimum.
- in the point $b = b_{\text{max}}/2$ the maximum potential drop across the polar cap reaches its minimum value $\Delta V_{\text{max}} = 0.086$.

The reason for such behaviour of the potential is easy to understand from the Fig. B1 in Appendix B. The critical points where $V(\psi)$ changes its behaviour are the points where the line $a = 0$ intersects the boundaries of the regions I,II,II, and IV.

The angular velocity of the open magnetic field lines is

$$\beta^c(\psi) = \frac{2b}{2 - \psi} \quad (47)$$

Distribution of the corresponding angular velocity is shown in Fig. 6. For $b > 1$ the angular velocity of rotation of all open magnetic field lines is larger than the angular velocity of the NS. For $b < 1/2$ all magnetic field lines rotate slower

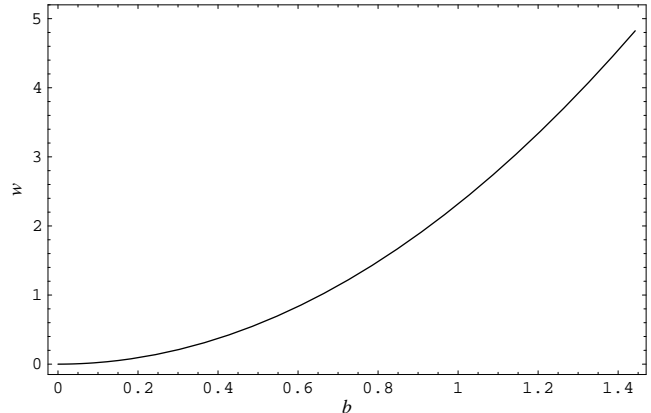


Figure 8. Spindown rate of an aligned rotator normalised to the spindown rate in the Michel solution for magnetosphere configurations with a constant current density across the cap as a function of the current density in the polar cap (parameter b).

that the NS. For $1/2 < b < 1$ some open field lines near the rotation axis rotates slower than the NS, the other open field lines rotates faster than the NS.

The current density distribution in terms of the GJ current density is

$$i^c(\psi) = \frac{1}{4}(2 - \psi)^2, \quad (48)$$

and it doesn’t depend on the value of the parameter b . The current density is always sub-Goldreich-Julian, except the rotation axis, where it is equal to the GJ current density.

The normalised spindown rate for the considered case has simple quadratic dependence on the current density

$$w^c = 6(\log 4 - 1)b^2. \quad (49)$$

This dependence is shown in Fig. 8. The energy losses in configuration with a constant current density could not be higher than ≈ 4.82 of the energy losses in the corresponding Michel solution.

The case $b = 1$ is worth to mention separately, as it is “the most natural” state for the space charge limited particle flow, for which the current density at the surface on the NS is equal to the corotational GJ current density. In Figs. 5, 6, 7 the lines corresponding to this case are labelled with “3”. The maximum potential drop for the configuration with the current density distribution being equal to the corotational GJ current density is $\Delta V_{\text{max}} = 0.386$ and the angular velocity of the open field lines varies from 1 at the rotation axis to 2 at the polar cap boundary.

4.6.2 Configurations with the smallest potential drops

As the next example we consider the case when the maximum potential drop across the polar cap for a fixed value of either a or b is minimal. The points corresponding to such values of parameters are shown in Figs. 2, 3, 4 by the thick grey line. Equation for this line in the plane (a, b) is derived in Appendix B, equation (B1). In some sense this is an optimal configuration for the cascade zone, because for a fixed value of the current density at some magnetic field line such configuration requires the smallest potential drop

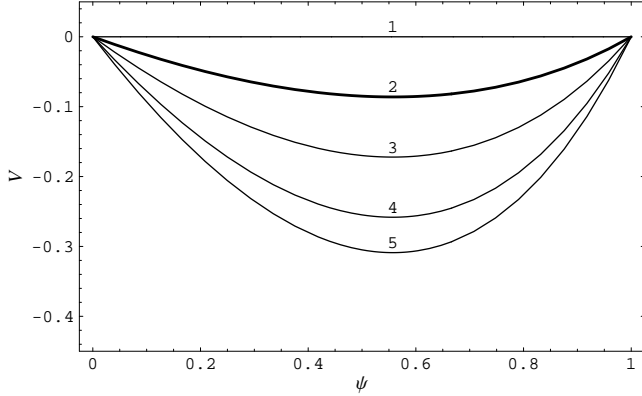


Figure 9. Electric potential in the polar cap of pulsar as a function of the normalised flux function ψ for magnetosphere configurations with the smallest potential drop across the cap. In all cases V_0 is set to zero. Numbered lines correspond to the following values of a : 1 — $a = -1$ (Michel's solution); 2 — $a = 0$ (solution with a constant current density); 3 — $a = 1$; 4 — $a = 2$; 5 — $a = 1/(\log 4 - 1)$.

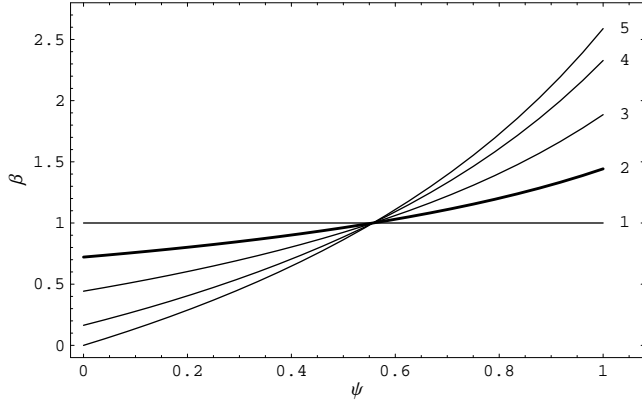


Figure 10. Normalised angular velocity of the open magnetic field lines as a function of the normalised flux function ψ for magnetosphere configurations with the smallest potential drops across the cap. Labelling of the curves is the same as in Fig. 9.

among the other admitted configurations. The accelerating potential for the considered class of configurations is

$$V^s(\psi) = V_0 - (a + 1) \left\{ \psi + \log \left[\left(1 - \frac{\psi}{2} \right)^{\frac{1}{\log 2}} \right] \right\}. \quad (50)$$

The potential is shown as a function of ψ in Fig. 9 for several particular cases assuming for the sake of simplicity zero potential drop at the polar cap boundary. The potential has always a minimum at the point

$$\psi_{\min}^s = 2 - \frac{1}{\log 2} \simeq 0.557, \quad (51)$$

the position of this minimum does not depend of the values of a, b . The minimum value of the maximal potential drop across the cap, $\min(\Delta V_{\max}) = 0$, is achieved at the left end of the grey line, at the point ($a = -1, b = 1$) corresponding to the Michel solution. The maximum potential drop across the gap for this class of configurations, $\max(\Delta V_{\max}) = 0.309$,

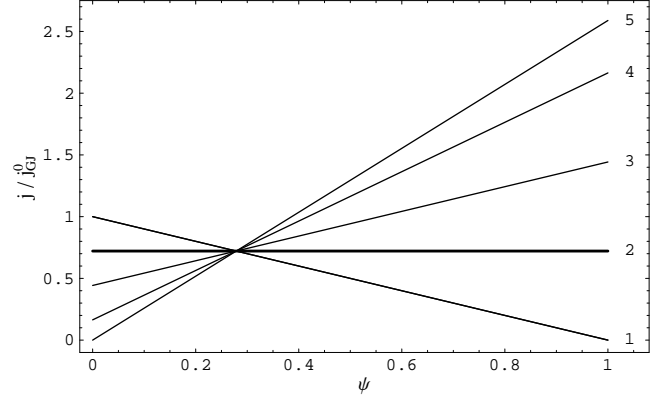


Figure 11. Current density as a function of the normalised flux function ψ for magnetosphere configurations with the smallest potential drops across the cap. Labelling of the curves is the same as in Fig. 9.

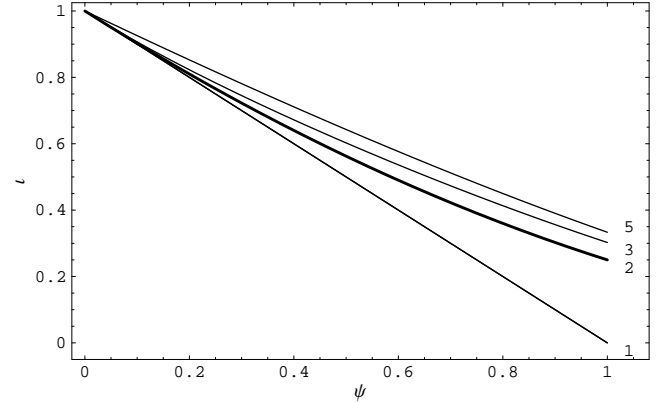


Figure 12. Ratio of the actual current density to the GJ current density ι as a function of the normalised flux function ψ for magnetosphere configurations with the smallest potential drops across the cap. Labelling of the curves is the same as in Fig. 9.

is achieved at the right end of the grey line, at the point ($a = 1/(\log 4 - 1), b = 0$).

The angular velocity of the open field lines is

$$\beta^s(\psi) = \frac{a + 1}{(2 - \psi) \log 2} - a \quad (52)$$

Distribution of $\beta^s(\psi)$ is shown in Fig. 10. Before the minimum point ψ_{\min}^s β is not greater than 1, after that point β is not smaller than 1. With increasing of the maximum potential drop the variation of the angular velocity across the polar cap becomes larger.

The current density distribution in the considered case has the form

$$j^s(\psi) = a\psi + \frac{a(1 - \log 4) + 1}{\log 4}. \quad (53)$$

That distributions is shown in Fig. 11. All curves pass through the point $\hat{\psi} = 1 - 1/\log 4$, where the current density is $j^s(\hat{\psi}) = j_{GJ}^0/\log 4$.

The current density distribution in terms of the

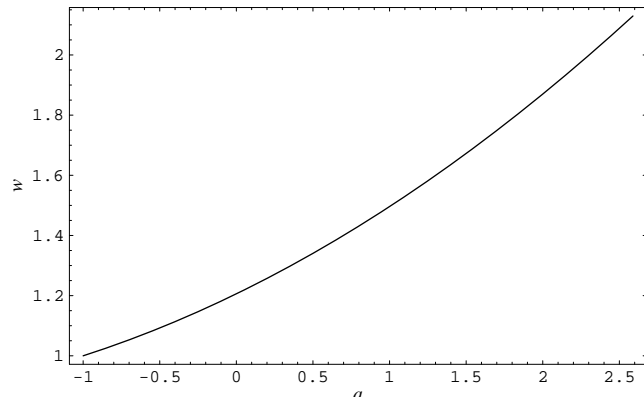


Figure 13. Spindown rate of an aligned rotator normalised to the spindown rate in the Michel solution for magnetosphere configurations with the smallest potential drops across the polar cap as a function of the parameter a .

Goldreich-Julian current density is

$$i^s(\psi) = \frac{(\psi - 2)^2 [(\psi - 1)a \log 4 + a + 1]}{\psi(4 - \psi)a \log 4 + 4a(1 - \log 4) + 4}, \quad (54)$$

It monotonically decreases from 1 at the rotation axis to its minimum value at the PC boundary. This minimum value is in the range $[0, 1/3]$, the lowest value corresponds to the left end of the grey curve (the Michel solution), the upper value corresponds to the right end of the grey line. The outflow is sub-GJ everywhere except the rotation axis.

The normalised spindown rate for the considered case is

$$w^s = \frac{1}{2 \log^2 2} \{ [2 \log^2 2 - 3(1 - \log 2)] a^2 - 3(2 - 3 \log 2)a - 3(1 - 2 \log 2) \}. \quad (55)$$

It is shown as a function of the parameter a in Fig. 13. We see that for the considered configuration the spindown rate as a function of the parameter a increases more slowly than the spindown rate for configurations with a constant current density as a function of b , cf. Fig. 8. The energy losses could not be higher than ≈ 2.13 of the energy losses in the corresponding Michel solution.

5 DISCUSSION

The main aim of this paper was to study the range of admitted current density distributions in force-free magnetosphere of an aligned rotator. Taking into account that this subject was not studied in details before, the linear model used in this work is in our opinion an adequate approach to the problem. The knowledge of the magnetosphere behaviour in response to different potential drops in the polar cap would be very useful for future modelling of non-stationary polar cap cascades. This formalism could be used as a tool allowing to judge quickly whether a particular model of the polar cap cascades is compatible with the force-free magnetosphere or not. It may also give a clue how the magnetosphere would respond to a particular current density distributions obtained at some step in course of numerical solution. Although the

analytical model presented here needs to be refined in numerical simulations, the presence of some analytical relations should be very handy for numerical cascade modelling.

We have considered here a simple case when the current density in the polar cap of pulsar is a linear function of the magnetic flux. However, the generalisation of the model to the case of a more complicated shape of the current density distribution is straightforward. One should proceed with the steps described at the beginning of the Section 3 for the desired form of the current density distribution. The resulting equation for the electric potential will be an ordinary differential equation, and numerical solution of such equation for any given current density will not be a problem.

The main conclusion we would like to draw from the presented results is that even for rather moderate potential drop in the acceleration zone the current density distribution can deviate significantly from the “canonical” Michel distribution, which is basically preserved for dipole geometry if all field lines corotates with the NS (see Paper I). In particular, a magnetosphere configuration with the constant current density at the level of 73 per cents of the Goldreich-Julian current density at the NS surface would require a potential drop in the acceleration zone of the order of 10 per cents of the vacuum potential drop. For time-dependent cascades this may be realised even for young pulsars. We should note however that for young pulsars the potential drop of the order of 10 per cents of the vacuum drop could cause overheating of the polar cap by the particles accelerated toward the NS (e.g. Harding & Muslimov 2001, 2002). In that sense such potential drop may be too large for young pulsars. On the other hand, without knowledge of the dynamics of non-stationary cascades it is in our opinion too preliminary to exclude the possibility of such configurations for young pulsars, as in non-stationary regime the heating of the cap may be not so strong as in stationary cascades (see Levinson et al. 2005).

We used split-monopole approximation for the poloidal current density distribution in the magnetosphere, which would produce an accurate results only for configurations with very small size of the corotating zone, less than the size of the light cylinder $x_0 \ll 1/\beta(\Psi_{pc})$, see Fig. 1. For the (most interesting) case when these sizes are comparable, results obtained in this work could be considered only as a zero approximation to the real problem. We should point out an important modification introduced by the dipole geometry of the magnetic field. For the dipole geometry there will be some magnetic field lines which bent to the equatorial plane at the light cylinder. For these field lines the second term⁵ on the r.h.s. of equation (4) will be negative, and in order to get positive current density along these lines a more steep dependence of β on ψ would be necessary. As a result the potential drop in the dipole geometry would be higher than it is obtained in our approximation. Figuratively speaking, in our model we could correct only for the decrease of the electric current density toward the polar cap boundary present in the Michel solution. On the other hand, if $\beta(\Psi_{pc}) > 1$, the size of the corotating zone can be less as well as greater⁶

⁵ which in the cylindrical coordinates (ϖ, ϕ, z) is $2\beta\partial_\varpi\Psi$

⁶ for the closed magnetic field lines the angular velocity is Ω and they are still inside *their* light cylinder; the adjustment of the

then the light cylinder radius at the last open field line. In the latter case there should be less magnetic field lines which bent toward the equatorial plane, than in the first case, cf. Fig. 1 cases **I** and **II**. Hence, the correction introduced by the dipolar field geometry for some subset of our solutions would be non-monotonic as the size of the corotating zone x_0 increases. So, there is still possibility that a moderate potential drop could allow a large variety of the current densities, although this issue needs careful investigation.

In this paper we ignored the electrodynamics of the polar cap zone. Although without a theory of time-depending cascades we cannot put more limits on the electric potential than the one we used in Section 2.2, there is an additional limitation coming from the basic electrodynamics. Namely, the accelerating potential near conducting walls, which the current sheet at the polar cap edge is believed to be, should approach zero. However, we could speculate that there is a thin non-force-free zone at the edge of the polar cap where the adjustment of the potential happens. In other words, the return current and the actually nearly equipotential region may occupy not the whole non-force-free zone. Because of this that limitation would not eventually restrict our solutions.

At the end we would like to discuss briefly the issue with the pulsar braking index. If the inner pulsar magnetosphere is force-free, then the spindown rate of an aligned pulsar as a function of angular velocity will deviate from the power law $W \propto \Omega^4$ if the size of the corotating zone or/and the distribution $\beta(\psi)$ change with time. The assumption that these “parameters” are time dependent seems to us to be natural, because with the ageing of pulsar the conditions in the polar cap cascade zone change and the magnetosphere should adjust to these new conditions. In the frame of our model we could make some simple estimations how the braking index of pulsar is affected by the changes of these two “parameters”.

As an example we consider the case when the pulsar magnetosphere evolves through a set of configurations with a constant current density. The spindown rate for such configurations is

$$W \propto \Omega^4 \Psi_{\text{pc}}^2 b^2 \sim \Omega^4 x_0^{-2} b^2, \quad (56)$$

here we estimate Ψ_{pc} assuming dipole field in the corotation zone. If b and/or x_0 are functions of time, the spindown rate will be different from the spindown of a dipole in vacuum. If at some moment the dependence of the size of the corotating zone and the current density on Ω could be approximated as $x_0 \propto \Omega^\xi$ and $b_0 \propto \Omega^\zeta$ correspondingly, the braking index of pulsar measured at that time is

$$n = 3 - 2\xi + 2\zeta. \quad (57)$$

We see, that the deviation of the braking index from the “canonical” value being equal to 3 would be by a factor of two larger than the dependence of b and x_0 on Ω . The braking index could be smaller as well as larger than 3, depending on the sign of the expression $\zeta - \xi$. For instance, if in an old pulsar the potential drop increases and, as the consequence, the current density decreases, ζ is positive, and

angular velocity occurs in the current sheet, which is for sure a non-force-free domain.

the braking index could be *greater* than 3. We note, that there are evidences for such values of the braking index for old pulsars (Arzoumanian et al. 2002). On the other hand, if x_0 decreases with the time, as it was proposed in Paper I for young pulsars, the braking index would be less than 3. However even in this simple picture different trends may be possible. In reality the evolution of the pulsar magnetosphere will be more complicated and more steep as well as more gradual dependence of the braking index on the current density would be possible. This would results in a rather wide range of possible values of pulsar braking index.

ACKNOWLEDGMENTS

I acknowledge J. Arons, J. Gil, Yu. Lyubarsky and G. Melikidze for fruitful discussions. I would like to thank J.Arons for useful suggestions to the draft version of the article. This work was partially supported by the Russian grants N.Sh.-5218.2006.2, RNP.2.1.1.5940, N.Sh.-10181.2006.2 and by the Israel-US Binational Science Foundation

REFERENCES

- Al’Ber Y. I., Krotova Z. N., Eidman V. Y., 1975, *Astrophysics*, 11, 189
Arons J., 1979, *Space Science Reviews*, 24, 437
Arzoumanian Z., Chernoff D. F., Cordes J. M., 2002, *ApJ*, 568, 289
Beskin V., Gurevich A., Istomin Y., 1993, *Physics of the Pulsar Magnetosphere*. Cambridge University Press
Beskin V. S., 2005, ”Osesimmetrichnye stacionarnye techeniya v astrofizike” (Axisymmetric stationary flows in astrophysics). Moscow, Fizmatlit, *in russian*
Blandford R. D., Znajek R. L., 1977, *MNRAS*, 179, 433
Bucciantini N., Thompson T. A., Arons J., Quataert E., Del Zanna L., 2006, *MNRAS*, 368, 1717
Contopoulos I., 2005, *A&A*, 442, 579
Contopoulos I., Kazanas D., Fendt C., 1999, *ApJ*, 511, 351
Fawley W. M., 1978, PhD thesis, AA(California Univ., Berkeley.)
Goldreich P., Julian W. H., 1969, *ApJ*, 157, 869
Goodwin S. P., Mestel J., Mestel L., Wright G. A. E., 2004, *MNRAS*, 349, 213
Gruzinov A., 2005, *Phys.Rev.Lett.*, 94, 021101
Harding A. K., Muslimov A. G., 2001, *ApJ*, 556, 987
Harding A. K., Muslimov A. G., 2002, *ApJ*, 568, 862
Komissarov S. S., 2006, *MNRAS*, 367, 19
Levinson A., Melrose D., Judge A., Luo Q., 2005, *ApJ*, 631, 456
Lyubarskij Y. E., 1992, *A&A*, 261, 544
McKinney J. C., 2006, *MNRAS*, 368, L30
Michel F. C., 1973a, *ApJ*, 180, 207
Michel F. C., 1973b, *ApJ Letters*, 180, L133
Michel F. C., 1991, *Theory of neutron star magnetospheres*. Chicago, IL, University of Chicago Press, 1991, 533 p.
Okamoto I., 1974, *MNRAS*, 167, 457
Ruderman M. A., Sutherland P. G., 1975, *ApJ*, 196, 51
Scharlemann E. T., Arons J., Fawley W. M., 1978, *ApJ*, 222, 297
Scharlemann E. T., Wagoner R. V., 1973, *ApJ*, 182, 951

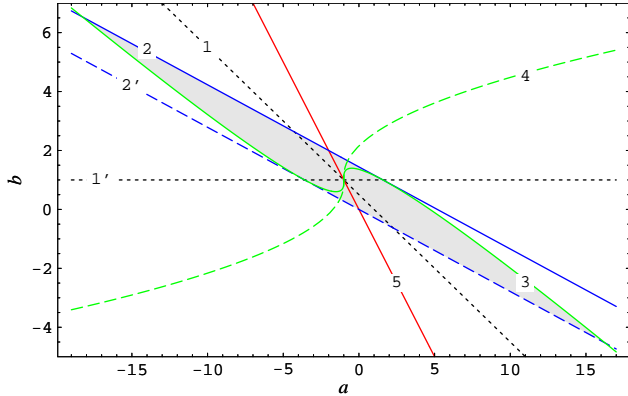


Figure A1. Value of parameters a and b admitted by the requirement that the maximum potential drop across the polar cap is less than the vacuum potential drop. Dotted lines **1** and **1'** show the boundary of the region where the potential has an extremum in the polar cap. Line **2** corresponds to $\Delta V_{10} = 1$, and **2'** - to $\Delta V_{10} = -1$. Line **3** show points when $|\Delta V_{1e}| = 1$, and **4** - $|\Delta V_{0e}| = 1$. Line **2'** corresponds to $b = -a$. The resulting admitted region is shown by the grey colour. See text for the explanations.

Spitkovsky A., 2006, ApJ Letters, 648, L51

Timokhin A. N., 2006, MNRAS, 368, 1055

Timokhin A. N., 2007, Ap&SS, in press, astro-ph/0607165

APPENDIX A: ADMITTED CURRENT DENSITY

The second derivative of $V(\psi)$ in respect to ψ is

$$V''(\psi) = 2 \frac{a+b}{(2-\psi)^2}. \quad (\text{A1})$$

For fixed a and b the second derivative never changes the sign, hence, $V(\psi)$ has a single extremum. If $a+b > 0$, $V(\psi)$ has a single minimum; in the plane (a, b) shown in Fig. A1 these points lie left to the line **5**. If $a+b < 0$, $V(\psi)$ has a single maximum, such points lies to the right of the line **5** in Fig. A1. The potential reaches its extremum value at the point

$$\psi_{\text{ex}} = 2 \frac{1-b}{a+1}, \quad (\text{A2})$$

This point lies in the interval $[0, 1]$ if

$$\begin{aligned} 1 \geq b \geq \frac{1-a}{2}, & \quad \text{for } a > -1; \\ 1 \leq b \leq \frac{1-a}{2}, & \quad \text{for } a < -1. \end{aligned} \quad (\text{A3})$$

In Fig. A1 points where these conditions are satisfied lie between the lines **1** and **1'**, in the region where the angle between the lines is acute. The line **1** corresponds to the values of a, b when the extremum of the potential is reached at the polar cap boundary. For a, b lying on the line **1'** the potential reaches the extremum at the rotation axis.

If ψ_{ex} is outside of the interval $[0, 1]$, $V(\psi)$ is a monotone function of ψ in the polar cap of pulsar and the maximum potential drop is the potential drop between the edge of the

polar cap and the rotation axis. In that case the condition (9) takes the form

$$|\Delta V_{10}| \leq 1, \quad (\text{A4})$$

where $\Delta V_{10} \equiv V(1) - V(0)$ is the potential drop between the the boundary of the polar cap and the rotation axis. In terms of the parameters a, b it can be written as

$$a \frac{1 - \log 4}{\log 4} \leq b \leq \frac{1}{\log 2} + a \frac{1 - \log 4}{\log 4}. \quad (\text{A5})$$

In Fig. A1 points satisfying this condition lie between the lines **2** and **2'**. In the region, where the angle between the lines **1** and **1'** is abuse (here the point ψ_{ex} is outside of the interval $[0, 1]$) the lines **2** and **2'** sets the boundaries for admitted values of the parameters a and b .

If the electric potential reaches its extremum value inside the polar cap, the maximum potential drop is achieved either between the extremum point and the edge of the polar cap, or between the extremum point and the rotation axis. In that case the condition (9) takes the form

$$\max(|\Delta V_{10}|, |\Delta V_{0e}|, |\Delta V_{1e}|) \leq 1, \quad (\text{A6})$$

where $\Delta V_{0e} \equiv V(0) - V(\psi_{\text{ex}})$ is the potential drop between the rotation axis and the point ψ_{ex} , and $\Delta V_{1e} \equiv V(1) - V(\psi_{\text{ex}})$ is the potential drop between the polar cap boundary and the point ψ_{ex} . Expression for the extremum value of V is non-linear in respect to a, b :

$$V(\psi_{\text{ex}}) = V_0 - 1 + a + 2b - 2(a+b) \log \left[\frac{2(a+b)}{1+a} \right], \quad (\text{A7})$$

and condition (A3) in terms of a, b should be evaluated numerically. For a fixed a the derivatives of ΔV_{0e} and ΔV_{1e} in respect to b are

$$\frac{d\Delta V_{0e}}{db} = 2 \log \left(\frac{a+b}{1+a} \right) \quad (\text{A8})$$

$$\frac{d\Delta V_{1e}}{db} = 2 \log \left(\frac{a+b}{1+a} \right) + \log 4. \quad (\text{A9})$$

If $\psi_{\text{ex}} \in [0, 1]$ and condition (A3) is fulfilled, then $d\Delta V_{1e}/db$ is positive and $d\Delta V_{0e}/db$ is negative. So, for a fixed a when $\psi_{\text{ex}} \in [0, 1]$ ΔV_{0e} decreases and ΔV_{1e} increases with increasing of b .

In Fig. A1 the line **3** represents points where $|\Delta V_{1e}| = 1$, and the line **4** - the points where $|\Delta V_{0e}| = 1$. To the right of the line **5** $V(\psi)$ has a minimum, and the lines **3** and **4** represent points where $\Delta V_{1e} = 1$ and $\Delta V_{0e} = 1$ correspondingly. To the left of the line **5** $V(\psi)$ has a maximum, and here the lines **3** and **4** correspond to $\Delta V_{1e} = -1$ and $\Delta V_{0e} = -1$. The line **4** lies always outside of the region between lines **1** and **1'**, and, hence, the absolute value of the potential drop between the extremum point and the rotation axis $|\Delta V_{0e}|$ never achieves the vacuum potential drop when the extremum point is inside the interval $(0, 1)$.

ΔV_{1e} increases with increasing of b . So, below the curve **3** to the right of the line **5**, and above the curve **3** to the left of the line **5** $|\Delta V_{0e}|$ is less than 1. Hence, when $\psi_{\text{ex}} \in [0, 1]$ (a, b are in the area between the lines **1** and **1'**), the admitted values of a and b are limited by the lines **3** and **2'** to the left from the line **5**, and by the lines **2** and **3** to the right from the line **5**.

Combining all discussed restrictions we get the region of the admitted values of parameters a and b , which is shown in Fig. A1 by the grey area.

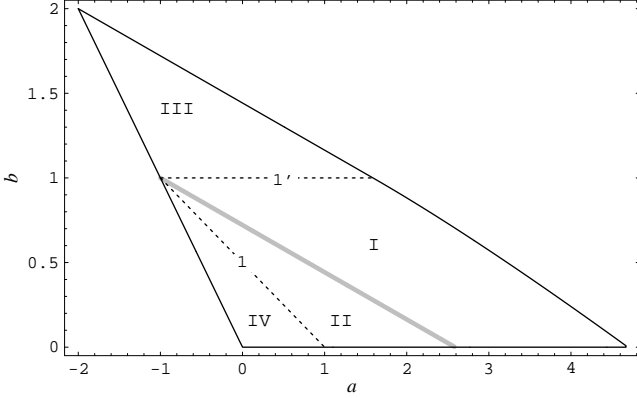


Figure B1. Region of admitted values of the parameters a and b corresponding to current densities being of the same sign as the Goldreich-Julian current density. The dotted line **1** shows points where $\Delta V_{1e} = 0$, the line **1'** - points where $\Delta V_{0e} = 0$. The thick grey shows points where $|\Delta V_{0e}| = |\Delta V_{1e}|$. In the region I - $\Delta V_{\max} = \Delta V_{1e}$, in the region II - $\Delta V_{\max} = \Delta V_{0e}$, in the regions III and IV - $\Delta V_{\max} = |\Delta V_{10}|$. See explanations in the text.

APPENDIX B: THE MAXIMUM POTENTIAL DROP ACROSS THE POLAR CAP

In Fig. B1 the dotted lines **1** and **1'** limit the region⁷ in the parameter space (a, b) where the potential in the polar cap is a non-monotone function of ψ and it has a minimum at some point $\psi_{\text{ex}} \in (0, 1)$, see Appendix A. In the regions III and IV the potential $V(\psi)$ is a monotone function of ψ .

The potential drop $\Delta V_{0e} \equiv V(0) - V(\psi_{\text{ex}})$ between the rotation axis and the point ψ_{ex} where $V(\psi)$ achieves its minimum value, for a fixed a decreases with increasing of b . For a, b at the line **1'** ψ_{ex} is at the rotation axis, and $\Delta V_{0e} = 0$ there. The potential drop $\Delta V_{1e} \equiv V(1) - V(\psi_{\text{ex}})$ between the polar cap boundary and the point ψ_{ex} for a fixed a increases with increasing of b . For a, b on the line **1** ψ_{ex} is at the polar cap boundary and $\Delta V_{1e} = 0$. So, ΔV_{0e} increases in the direction from the line **1'** to the line **1**, and ΔV_{1e} increases in the direction from the line **1** to the line **1'**.

Along some line between lines **1'** and **1** the potential drops ΔV_{0e} and ΔV_{1e} become equal. This means also that the potential drop $\Delta V_{10} \equiv V(1) - V(0)$ between the polar cap edge and the rotation axis is zero there. Equation for this line is obtained easily from the requirement $\Delta V_{10} = 0$:

$$b = \frac{1}{\log 4} + a \frac{1 - \log 4}{\log 4}. \quad (\text{B1})$$

This line is shown in Fig. B1 by the thick grey line. Above the grey line in Fig. B1 $\Delta V_{1e} > \Delta V_{0e}$, and below it $\Delta V_{1e} < \Delta V_{0e}$. Hence, the line given by eq. (B1) is the line where the maximum potential drop across the polar cap achieves its minimum value for fixed a or b .

Taking all this into account we conclude, that the maximum potential drop across the polar cap ΔV_{\max} is equal to the following potential drops: in the region I - to ΔV_{1e} , in the region II - to ΔV_{0e} , in regions III and IV - to $|\Delta V_{0e}|$.

APPENDIX C: ENERGY OF THE ELECTROMAGNETIC FIELD IN SPLIT-MONOPOLE CONFIGURATION

The energy density of the electromagnetic field in the magnetosphere is

$$w = \frac{1}{8\pi} (E^2 + B_{\text{pol}}^2 + B_{\phi}^2). \quad (\text{C1})$$

For the split monopole solution when $\Psi = \Psi_{\text{pc}}(1 - \cos \theta)$ the non-zero components of the electric and magnetic fields are

$$E_{\theta} = -\frac{\mu}{R_{\text{LC}}^3} \Psi_{\text{pc}} \beta \frac{\sin \theta}{r} \quad (\text{C2})$$

$$B_r = \frac{\mu}{R_{\text{LC}}^3} \frac{\Psi_{\text{pc}}}{r^2} \quad (\text{C3})$$

$$B_{\phi} = -\frac{\mu}{R_{\text{LC}}^3} \Psi_{\text{pc}} \beta \frac{\sin \theta}{r}. \quad (\text{C4})$$

So, the electric field is equal to the toroidal magnetic field, $E_{\theta} = B_{\phi}$. The total energy of the magnetosphere is then

$$\mathcal{W} = \frac{1}{8\pi} \int (B_r^2 + 2E_{\theta}^2) dV \quad (\text{C5})$$

On the other hand, the energy losses are

$$W = \int_{4\pi} c \frac{[\mathbf{E} \times \mathbf{B}]_r}{4\pi} d\tilde{\Omega} = \int_{4\pi} c \frac{E_{\theta}^2}{4\pi} d\tilde{\Omega}, \quad (\text{C6})$$

where $\tilde{\Omega}$ is a solid angle. Using equations (C6), (C3) we can rewrite the expression (C5) for the total energy of electromagnetic field as

$$\mathcal{W} = \frac{W_{\text{md}}}{c} \times \left[\frac{\Psi_{\text{pc}}^2 R_{\text{LC}}^2}{2} \left(\frac{1}{R_{\text{NS}}} - \frac{1}{R} \right) + W(R - R_{\text{NS}}) \right], \quad (\text{C7})$$

where R is the size of the magnetosphere (where its dynamics is determined by the central object). The first term represents the total energy of the poloidal magnetic field and it is the same for all configurations with different potential drops. The second term, being the sum of the energies of the electric field and the toroidal component of the magnetic field is different for different values of the accelerating potential. It is directly proportional to the energy losses in a particular configuration.

⁷ regions I and II together